Proceedings of ASME Turbo Expo 2018: Turbomachinery Technical Conference and Exposition
GT2018
June 11-15, 2018, Oslo, Norway

GT2018-75548

ANALYSIS OF PARAMETERS INFLUENCING BUILD ACCURACY OF A SLM PRINTED COMPRESSOR OUTLET GUIDE VANE

Adetayo Otubusin, Paul Wood
Institute for Innovation in Sustainable Engineering
University of Derby
Derby
United Kingdom

John Appleby, Rafael Adamczuk[1]
Florida Turbine Technologies (UK) Ltd.
Derby
United Kingdom
Email: radamczuk@fttukltd.co.uk

ABSTRACT

The paper describes the manufacture of an outlet guide vane (OGV) of jet engines by the Selective Laser Melting (SLM) process, in view of current challenges for conventional machining approaches such as; high airfoil profile tolerances, limited tooling access and hard to machine materials like nickel-chromium-based super alloys. Within this paper, analysis was conducted to investigate the influence of build parameters on possible distortion during printing that affect the build accuracy. These parameters include the part orientation on the build plate, thickness change to the flanges and the positioning of the support structure of each part. The configurations are 3D printed using the SLM approach. The chosen material is IN625. The printed parts are 3D scanned and the results are compared to the original CAD design. The results confirmed the presence of distortions in printed parts and the effect of parameter changes. Furthermore, it was shown that improvements to the print parameters are necessary to achieve a satisfactory profile tolerance.

NOMENCLATURE

Abbreviations.

AM	Additive Manufacturing
CAD	Computer Aided Design
CAE	Computer Aided Engineering
CNC	Computer Numerical Control
LE	Leading Edge
OGV	Outlet Guide Vane
SLM	Selective Laser Melting
TE	Trailing Edge

INTRODUCTION

Jet engine developments are usually geared towards achieving a higher efficiency, lower polluting emissions, greater stability and adaptability [1], hence making testing necessary and as such the need for producing test rigs. Test rigs are usually expensive, one off assemblies, requiring the compliance of the manufacturing tolerances in the production design. The complex and one off character of the parts paired with short lead times makes machining of the components particularly challenging. This paper focuses on the application of additive manufacturing (AM), specifically the Selective Laser Melting (SLM) to the manufacture of an Outlet Guide Vane (OGV) in an IN625 super alloy. The OGV is a last stator row in a compressor which serves to eliminate the tangential component of the air flow [2], deaccelarete the flow and increase the pressure. The vanes have an airfoil shape to direct the tangential flow from the high-pressure compressor into an axial flow with minimal pressure loss [3, 4].

The established route to manufacture an OGV uses CNC machining of a one piece ring, pre-formed by hot isothermal forging process. Nickel based super alloys which includes Inconel 625, is classified as hard to machine materials and presents many technical challenges in machining. A significant challenge in machining an OGV from a forged Nickel based alloy is control of residual stress together with tool and work piece deflection that needs to be compensated during the programming of the tool paths. In the roughing stage, the machining strategy must be developed to minimize machining induced stresses and account for the residual stress present in the forging. This requires a managed process of applying a small depth of cut sequentially from both faces of the OGV to avoid distorting the ring. The distortion type is typically characterized as 'curl up' if the machining process is not managed in the correct way. The cycle of applying small

[1] *Address all correspondence to this author.

depths of cut sequentially from both faces is repeated until the space between the vanes is removed. Witness marks or lines on the vane surface where the cutter breaks through to create the space between the vanes, together with machining surface aberrations arising from the roughing stage are removed in subsequent finishing stages. An undesirable feature of the machining process is the high waste material generated. [5] observed that traditionally, aerospace manufacturing, for example, "may generate more than 90 % in waste material that cannot be reused readily" by machining parts down to size from large metallic blocks.

Another challenge in the manufacture of test rig components such as an OGV is that the component must be manufactured right first time, which incurs higher cost and longer lead time to mitigate risk in manufacturing. For these reasons the SLM may offer an alternative route to manufacture such parts. A powder bed AM process enables the printing of parts on a build plate, by locally melting metal powder layer by layer in an inert atmosphere and fusing the powder particles together to manufacture a homogenous solid structure [5]. The appeal in the SLM process is that it can manufacture complex shapes with little waste, relatively low energy usage and short delivery lead times in comparison to long programming and trial phases of the conventional route [6].

With the leap in technological advancement in recent times, there is an increasing interest in the AM process as a leading candidate for alternative metal manufacturing process of complex geometric designs [5]. Specific aerospace components applications of AM technology has since been investigated. Such application includes; using AM technology to repair burners in the annular combustors of gas turbine engines like the SGT-800 which would normally be repaired by conventional methods of cutting and welding [7]. [8] used the technology to produce a high-pressure nozzle guide vane with complex internal cooling system and conducted a laboratory test to assess its thermal performance as a means of predicting the performance of the cast alternative. Stator heat shields for hot gas path was also designed and printed using the technology, leading to a reduction in part volume, and the applied stock for conventional finish machining, hence, allowing cost and time savings [9]. Can-combustor components and six air blast fuel nozzles were also manufactured using the AM technology in a development program that was looking at advancing the state of art in Unmanned Aerial Vehicle power systems [10].

Among the disadvantages of additive manufacturing which includes the SLM process is surface finish and part distortion arising from the design process parameters selected which include; location and number of the part build supports, part orientation, laser power, powder particle size, scan/build speed etc. [11]. As a result, there is a need to establish the capability of the SLM process as an alternative route to manufacture an OGV within the required tolerances.

In this paper, a representative OGV was designed. Parts were then manufactured using SLM with variations to the applied process parameters. The resulting parts were scanned and inspected using the GOM laser scanning system with a view to optimizing the build process.

DESIGN APPROACH FOR OGV DEMONSTRATOR

The OGV was chosen as the demonstrator component for this project. The demonstrator is based on a full-sized part of approximately 600 mm external diameter made from a nickel-based super alloy. The basis of design is to have a demonstrator which truly represents the complex geometric characteristics, manufacturing tolerances and hence all the challenges faced in the manufacture of a full size OGV.

Airfoil Selection

Considerations were given for certain parameters in the selection of airfoil. These include the chord length, maximum airfoil thickness and camber. These parameters were noted for the airfoils across the radial heights. NACA 6-series profiles as shown Figure 1 are used in compressor stages of aero-engines and this forms the baseline for the airfoil selection [12, 13]. A NACA 63-2007 profile was selected across the 20 % and 80 % radial height of the airfoil and a NACA 63-1807 profile was selected at 50 % radial height.

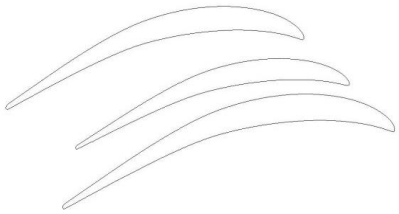

FIGURE 1 GEOMETRY OF 2D AIRFOILS OF NACA-6 SERIES

Design Drivers

The design intent involves the generation of suitable airfoil profiles, which match the characteristics of the airfoils within an OGV of a commercial engine. 140 vanes were patterned circumferentially within the endwalls and equally spaced. This ensures that the spacing between the airfoils are representative of the current manufacturing challenges. The distance between airfoils is roughly 6.5 mm.

The inner and outer endwall diameters were designed to match the full-size component. The endwall profiles were ignored for the purpose of this project, hence not included in the design of the OGV demonstrator, but rather assumed to be straight. A fillet of 1.7 mm was added to all joints between airfoils and wall, and the edges on the flanges.

CAD Design

In order to get a more rounded trailing edge, the airfoil was designed to have a 5 mm longer chord length and then trimmed off. With an annulus gap of 20 mm, the airfoils were then stacked from 0 % to 100 % respectively**.** The axial length of the endwall, which determines the thickness of the OGV was developed by taking into account the maximum chord length, and the fillet radius, giving a length of about 40mm.

Table 1 shows a list of the geometry data used to design the OGV demonstrator along with important manufacturing tolerances that have been assigned to the demonstrator part. A segment of the full-size component seen in Figure 2, consisting of five vanes and four flow passages was developed to enable feasibility evaluations of practical size and cost, and to find solutions to achieve an acceptable build accuracy. Three further configurations seen in Figure 3 to Figure 4 were also designed to study the influence of flange positioning and wall thickness on print accuracy.

FIGURE 2 OGV WITH 5 MM THICKNESS

FIGURE 3 OGV WITH 2.5 MM THICKNESS

FIGURE 4 OGV WITHOUT FLANGE

FIGURE 5 OGV WITH MID FLANGE

TABLE 1 OGV GEOMETRY DATA

Outer Diameter of Outer Flange (mm)	605
Inner Diameter of Inner Flange (mm)	465
Wall Thickness (mm)	5
Flange Thickness (mm)	5
Through Hole Diameter (mm)	10
Number of Vanes	140

EXPERIMENTAL APPROACH

Additive Manufacturing

The AM process starts by arranging the parts on a build plate as well as including the required support structures added to the part. The parts were initially printed with a 45° orientation, see Figure 6. This was the angle that ensures that minimal supports were required. It was also necessary to ensure that no support structures where needed on the airfoils. The removal of the support structures after print would distort the thin airfoil profile, and equally leave rough patches behind when supports are detached. The build plate also had 3 test pieces oriented at xy-planar 0°, 45° and 90° of the build plate. They are to be used for the calibration of Computer Aided Engineering (CAE) software that will be used to simulate the print process and predict possible distortions in prints at a later stage. The arrangement of parts on the build plate seen in Figure 6 is such that there will be an easy access for the EDM machine to fully detach the parts, as well as partly cut the calibration test pieces as required without needing to cut the plate in half, hence wasting the baseplate. The printing would typically last a couple of hours depending on the volume of print. Upon completion, the parts would then be first stress-relieved and later detached from the build plate.

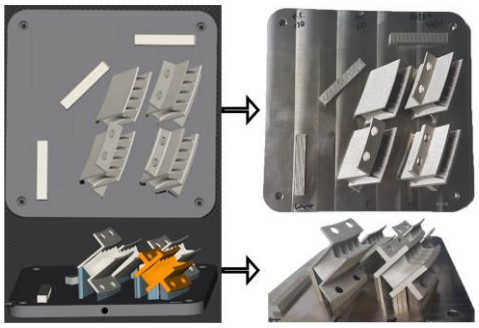

FIGURE 6 SAMPLE OF A BUILD LAYOUT AND ITS RESULTANT PRINT

The manufacturing trials were performed using a Renishaw AM250 SLM machine. This machine will create a homogenous solid metal component using laser energy to melt the powder layer by layer [14]. The volume energy (E_V) shown in Eqn. (1) describes the energy required to generate parts. This is represented mathematically as;

$$E_v = \frac{P}{vhd} \quad (1)$$

where P is the laser power, v is scan speed, h is hatch distance, and d is the layer thickness [15]. For the purpose of this research, the volume energy was not considered. This is partly because the SLM system by Renishaw is designed to vary the volume energy depending on the layers and surface area of sections being printed, and so the values of the parameters will vary as the scan moves from the core of each layer thickness to the surface boundary. The AM250 has a build volume of 250 mm x 250 mm x 300 mm, hence limiting the size of a part that

can be built. It has a capability of producing parts in a range of materials, and for the purpose of this project, IN625 powder having a particle size of 15-45 µm was used in the machine. It was supplied and certified by Renishaw to a tight specification to minimize batch-to-batch variations. The chemical composition of the powder can be seen in Table 2. In order to complete the build, the machine parameters in Table 3 were used.

TABLE 2 CHEMICAL COMPOSITON OF IN625 POWDER (WT. %)

Ni	Cr	Mo	Fe	Nb	Co	Mg	Si	Al
Bal	20	8	5	3.15	1	0.5	0.5	0.4

Al	Ti	C	Tn	Ni	O	Ph	S
0.4	0.4	0.1	0.05	0.02	0.02	0.015	0.015

TABLE 3 SLM MACHINE SETTING

PARAMETERS	VALUE
Gas Atmosphere	Argon
Laser Power	200W max
Laser Beam Spot Size Diameter	70µm
Laser Pulse Frequency	8 kHz
Build Orientation	45°
Layer Thickness	50µm

Stress Relief

Residual stresses form as the melted materials solidify on the previous layer resulting in part distortion and unwanted material properties [11,15]. Currently, AM parts are heat treated to reduce the internal stresses, and as [16] found, additional advantages such as improvement of the mechanical behavior can also be achieved.

Two sets of builds were initially created, only one of which was stressed relieved and the other not, in order to qualify the effect of the process in achieving a higher geometric accuracy. Generally, parts can either be stress relieved before or after being detached from the baseplate, however, from literatures [17 - 19], it was decided that complex parts such as the OGV should be stress-relieved before EDM wire cut, to minimize the chance of deformation compounding in the part.

The parts were stress-relieved at a temperature of 565 °C for a period of one hour in an argon environment, followed by a slow cool to room temperature. This heat treatment was applied to the parts whilst they were still attached to the build plate.

Wire EDM

The wire Electrical Discharge Machining process is necessary to detach the OGV components from the build plate. A solid Brass wire of 0.25 mm diameter with a co-axial flushing and ambient temperature inside the tank was used for this purpose. The cut was performed on the support structures close to the base plate to detach the parts from the plate, and the support then manually removed from the part with care. The recast layer resulting from the EDM process is contained in the support structure and hence has no influence on the actual part. [20].

Measurement Setup

The printed OGV demonstrators were 3D scanned using the GOM ATOS triple scanning system. In order to ensure the consistency and accuracy of scan, photogrammetry technology with 2 reference scale bars having an average deviation of 0.85 µm was utilized to calibrate the system. With reference point markers placed in a non-uniform pattern around the part being scanned. The laser system uses this to identify the areas in the part and fixture, and the non-uniformity ensures that scanning system can identify different scanned areas with a high precision. The 3D data was measured with an average reference point deviation of 4.89 µm. The laser scanner scans the surface of the OGV demonstrator (point cloud data) and translates this into a CAD file.

The nominal CAD data was superimposed with the scanned data using a best fit alignment of the components or specified datum. Because of the geometry of airfoils and vanes, it is not always clear where start and finish points are on the shape, as such, a “best-fit” alignment of the airfoil section is used to align the scanned data and the nominal CAD. Airfoil inspection is usually based on sectional analysis, as such, cross-sections across the vanes were taken across the 20 %, 50 % and 80 % radial heights on each of the 5 vanes in the OGV demonstrators, to investigate the accuracy of the print to the nominal design. An example of this aligned CAD and cross-section showing the comparison is illustrated in Figures 7 - 9.

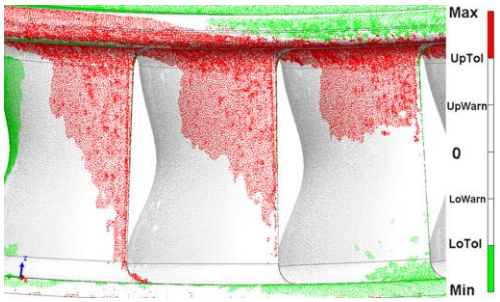

FIGURE 7 BEST-FIT ALIGNED CAD, SUCTION SIDE VIEW (UPPER TOLERANCE = 0.06 mm, LOWER TOLERANCE = -0.06 mm)

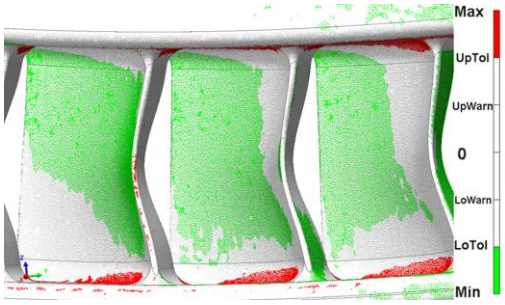

FIGURE 8 BEST FIT ALIGNED CAD – PRESSURE SIDE VIEW (UPPER TOLERANCE = 0.06 mm, LOWER TOLERANCE = -0.06 mm)

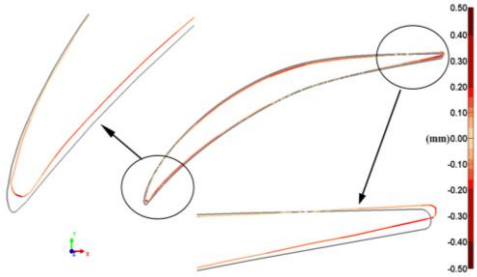

FIGURE 9 BEST FIT CROSS-SECTION AT 50 % HEIGHT OF VANE ZOOMED AT LEADING AND TRAILING EDGE

Results obtained were further analyzed, and this formed the basis of the design process/parameter optimization which was then fed into the start of the SLM print process to further increase the dimensional accuracy of the print. This is discussed in detail in the next section.

RESULTS AND DISCUSSION

A combination of several factors including; the melt pool dynamics, print orientation, coating process and part geometry among others all have an impact on the accuracy of the AM process [15]. Given the aerodynamic function of the OGV, the analysis of printed OGV segments focused on the airfoils, as these are the most important aspect of the part. For the purpose of inspection, cross sections were taken at three heights and the vanes on the OGV are numbered as seen in Figure 10.

Influence of Stress Relief

In order to evaluate the effect of stress-relief on SLM parts, the parts were printed on two builds with one of the builds going through a heat treatment cycle before getting detached from the build plate and the other detached as printed. The heat treatment is performed by heating up a furnace in an Argon atmosphere and placing the build inside for an hour, long enough to achieve the desired reduction in residual stress, and the slow cooled to room temperature to avoid formation of excessive thermal stresses.

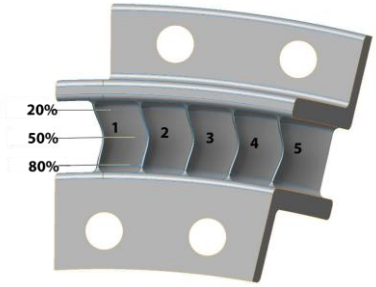

FIGURE 10 CROSS-SECTION POSITONS FOR INSPECTION OF OGV

At 50 % radial height cross-section results for the printed OGV as an example, Figure 11 shows that at the leading-edge, there is reduction in geometrical accuracy in the part that was not heat-treated as we move across vanes with a sharp drop in vane 5. This could possibly be as a result of the build orientation. The non-heat treated sample was undersized with an average accuracy of 82.5 % across all vanes. The sample that was stress-relieved however displays an increased average accuracy of 95 % which sits within the tolerance window.

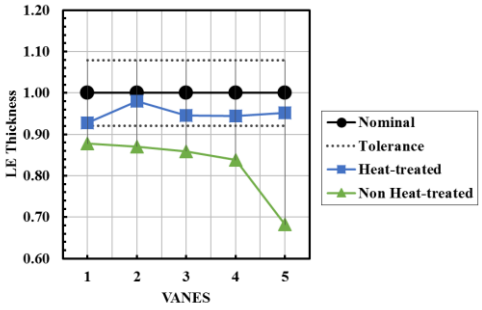

FIGURE 11 RELATIVE LEADING EDGE THICKNESS OF 2.5 MM WALL OGV AT 50 % RADIAL HEIGHT

Performing a similar analysis on the trailing-edge thickness, it can be seen from Figure 12 that the non-heat treated sample was undersized with 69.1 % accuracy and heat-treated sample having a 77.5 % accuracy, both of which

measured out of tolerance. The stress-relief process performed however still exhibits an increased average accuracy of 8.4 % across all vanes.

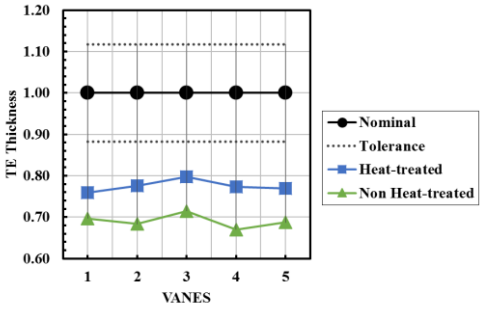

FIGURE 12 RELATIVE TRAILING EDGE THICKNESS OF 2.5 MM WALL OGV AT 50 % RADIAL HEIGHT

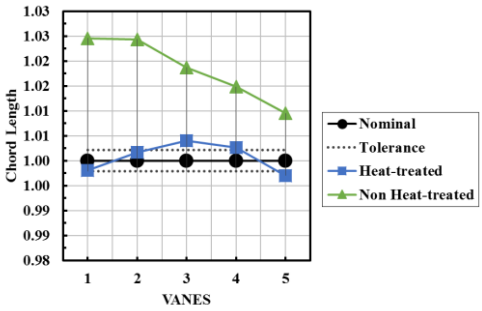

FIGURE 13 RELATIVE CHORD LENGTH OF 2.5 MM WALL OGV AT 50 % RADIAL HEIGHT

The effect of the heat treatment can also be seen in the chord length analysis in Figure 13. Here, we see that the stress-relief operation results in 100 % accuracy in chord length as opposed to the non-heat treated counterpart. There is an increasing trend in stagger angles in Figure 14 as we go from across vanes with a difference of 0.78° between Vanes 1 and 5 for the non-heated sample, whereas the heat treated sample has a reduced difference of 0.25°. It is observed that the stress relief process had an impact in reducing the deviation of the stagger angle from tolerance.

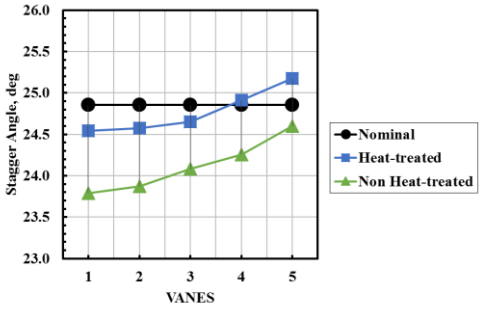

FIGURE 14 RELATIVE STAGGER ANGLE OF 2.5 MM WALL OGV AT 50 % RADIAL HEIGHT

A general trend which can be drawn across board is that the heat treatment operation has a positive influence in reducing the deviation of printed SLM parts from the nominal CAD. As a result of this, it was confirmed that stress-relief operation will be an important and standard operational step in achieving an improved accuracy for future SLM parts.

Influence of Angle Variation

Knowing from literature reviews that the build orientations generally have an effect on the build accuracy of prints, the optimal build orientation is important to achieve a higher geometric accuracy [15]. This will however differ depending on the geometry of the part. The OGV demonstrator was found to have a 10º window for which it can be printed. At this window, between 40° and 50°, the OGV can also be printed such that support structures will not be required on the vanes. This is very important as having supports on vanes will leave a disruption in the smooth profile of the vanes.

Following on from the result of the stress-relief's influence, the new build was conducted with a 2.5° step increment from 40° to 50°, and the finished print put through the stress-relief process before being detached from the build plate. Table 4 is the average result of measured parameters across all vanes for the OGV cross-section at 50 % radial height. Upon closer inspection, it can be seen that no conclusive effect can be drawn as to the significant influence of angle variation on these OGV demonstrators.

Influence of Geometry Variation - Wall Thickness

SLM prints will have a higher accuracy when the part have a larger cross-sectional area [15]. It is however only possible to change the geometry without changing the airfoils. Hence the following geometry variations namely; Wall thickness and Position of flange, were taken into account to investigate the influence they have on the build accuracy of the vanes.

TABLE 4 RELATIVE AVERAGE MEASUREMENTS ACROSS ALL VANES FOR 5MM WALL THICK OGV AT 50% RADIAL HEIGHT CROSS-SECTION

	40°	42.5°	45°	47.5°	50°	Design
LE Thickness	0.87	0.87	0.87	0.86	0.86	1.00
TE Thickness	0.76	0.75	0.72	0.72	0.74	1.00
Chord Length	1.00	1.00	1.01	1.00	1.00	1.00
Stagger Angle (°)	25.22	25.15	24.53	24.53	24.72	24.86

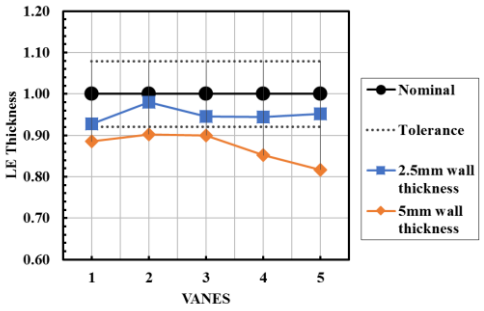

FIGURE 15 RELATIVE LEADING EDGE THICKNESS OF OGV AT 50% RADIAL HEIGHT WITH DIFFERENT WALL THICKNESS

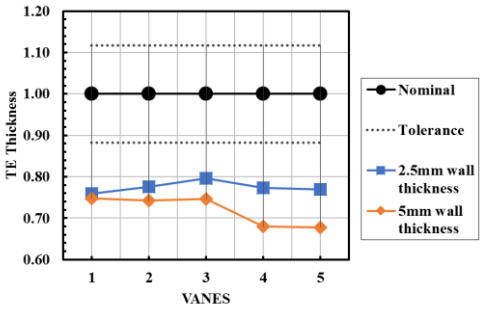

FIGURE 16 RELATIVE TRAILING EDGE THICKNESS OF OGV AT 50% RADIAL HEIGHT WITH DIFFERENT WALL THICKNESS

Figure 15 to Figure 18 show the result obtained from a comparison of wall thickness variaiton and sectioned at 50 % radial height. Generally, it can be seen that by reducing the wall thickness to 2.5mm, there is an improved accuracy in the geometry of the printed OGV demostrators. The leading-edge, trailing-edge, chord length and stagger angle were improved by an average of 7.9 %, 5.6 %, 1.2 % and 1 % across all vanes respectively as a result of this. The wall does have a structural function, as such, it limits the level to which the thickness can be reduced, and a minimum thickness will be adviced which delivers the best accuracy whilst still sufficient for the structural performance.

Commented [AR(1]: Why are we here suddenly in absolute values and not relative?!

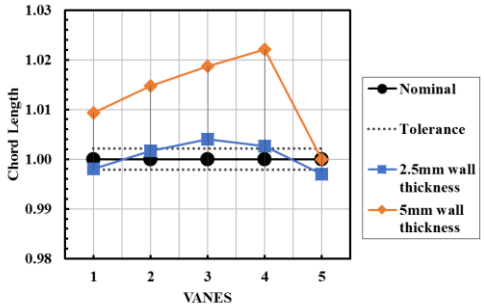

FIGURE 17 RELATIVE CHORD LENGTH OF OGV AT 50 % RADIAL HEIGHT WITH DIFFERENT WALL THICKNESS

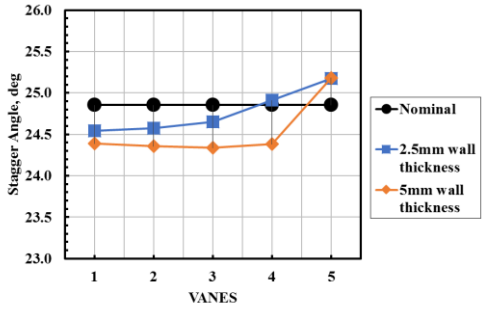

FIGURE 18 RELATIVE STAGER ANGLE THICKNESS OF OGV AT 50 % RADIAL HEIGHT WITH DIFFERENT WALL THICKNESS

Influence of Geometry Variation – Flange placement

Figure 19 to Figure 22 shows the result comparing the influence of flange placement on the OGV. The leading edge result obtained does not show a conclusive effect of the flanges, however the results are within the defined tolerance. All the trailing edge thicknesses in Figure 20 measured out of tolerance with the standard flange configuration having a slight improvement. Similarly in Figure 21, the standard flange configuration was on the average within tolerance, whereas the

two other configurations were out of tolerance and the part with mid-flange configuration displayed the highest deviation across all vanes. The stagger angles equally shows that the position of the flanges have an effect on the accuracy of the vanes with both standard and no flange configurations only 0.3 % inaccurate whereas the mid flange measures a 1.1 % inaccuracy on the average. All in all, it can be concluded that the flange position has a little effect on accuracy of across vanes with the standard flange variant having a slight advantage.

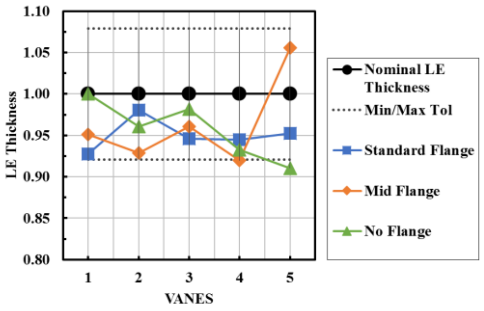

FIGURE 19 RELATIVE LEADING EDGE THICKNESS OF OGV FLANGE CONFIGURATIONS AT 50 % RADIAL HEIGHT CROSS-SECTIONS

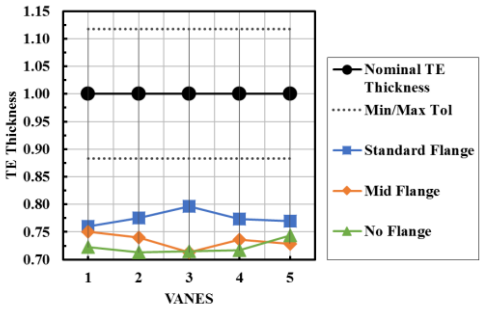

FIGURE 20 RELATIVE TRAILING EDGE THICKNESS OF OGV FLANGE CONFIGURATIONS AT 50 % RADIAL HEIGHT CROSS-SECTIONS

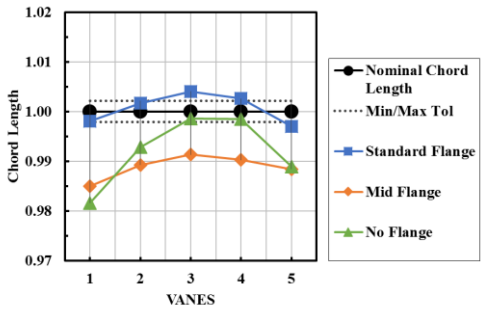

FIGURE 21 RELATIVE CHROD LENGTH OF OGV FLANGE CONFIGURATIONS AT 50 % RADIAL HEIGHT

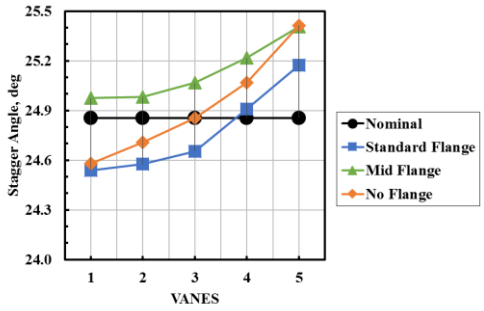

FIGURE 22 RELATIVE STAGGER ANGLE OF OGV FLANGE CONFIGURATIONS AT 50 % RADIAL HEIGHT

Profile Tolerance

A general trend observed in the results is that the profile cross-sections measured were typically undersize, which is consistent with the findings in [21] where the dimensional deviations of a metallic test article manufactured by laser sintering was inspected.

With regard to the build profile tolerance achieved, the maximum deviation was consistently observed on the pressure side of the cross section near the trailing edge which results in an undersized part ranging from 0.015 mm to 0.15 mm. This could be attributed to the airfoil overhang during the part build process which is not supported on the build platform. Further, the trailing edge is the thinnest section of the airfoil in which residual stress may readily develop during the build. In fact, the parts separated from the build plate having not been subject to a stress-relieving heat treatment and displaying the most pronounced deviation at the trailing edge section is consistent with the findings reported in [22]. Generally, [23] found that dimensional accuracy of metallic printed parts reduces as part height increases, this is also a possible factor that resulted in the

greater deviation experienced in the trailing edge section of the OGV as the print orientation seen in Figure 6 places the trailing edge higher up the build height. Overall, the SLM process achieved a high profile tolerance on an average across all vanes of the OGV prints. In Figure 23, with maximum average deviation recorded as 0.08mm which is only 0.02 mm out of tolerance. It can also be observed that the standard flange design has the best average profile tolerance.

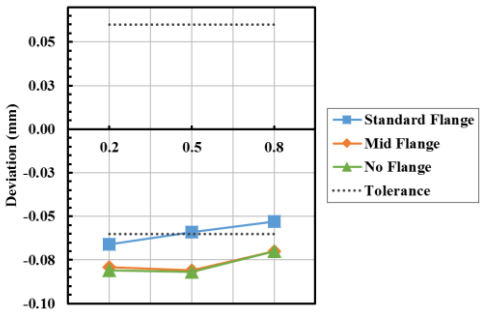

FIGURE 23 MEAN TOLERANCE DEVIATION OF VANES AT 20 %, 50 % AND 80 % RADIAL HEIGHT

CONCLUSIONS AND OUTLOOK

OGV segments were manufactured using the SLM process. The parts were printed with different parameters to study the influence of these parameters on the geometric accuracy of the vanes. Atos GOM scanning system was used to characterize the surface dimensions of the printed OGVs.

The obtained data confirmed that stress relieving the printed parts whilst still attached to the build plate is an important step to achieving a higher profile tolerance and accuracy, observing up to 12.5 % increase in accuracy, as all parts exhibited significant deviations when inspected as-built. Additionally, it was discovered that the build orientations has a negligible effect on the print accuracy for this particular component.

Analysis of the changes to the design geometry shows that the OGV prints with a higher accuracy of up to 8 % improvement when a reduced wall thickness is employed. Also, the position of flange has an effect on the achievable higher tolerance. On some areas, significant values of minimum and maximum deviations were recorded across the vanes, which was found to be as a result of the surface dips due to poor powder fusion on part's surface and overhangs around of the trailing edge, which was not supported for aerodynamic reasons. Overall, a high average profile tolerance was achieved.

The work presented only covers a limited aspect of consideration when using the AM process. For future work, the authors plan to include simulation studies to understand further, the causes of the distortions during print. Mechanical tests will also be carried out to understand the material properties of the printed IN625 when compared to the forged material.

ACKNOWLEDGMENTS

This research was jointly undertaken and sponsored by the Florida Turbine Technologies (FTT) and University of Derby under the Knowledge transfer partnership (KTP) program which is a UK government initiative, established to boost interaction between academia and industry.

We will like to acknowledge Charlie Birkett from Renishaw Plc, UK, and Dr. Gavin Williams from University of Derby for their input and advice throughout the course of this project.

REFERENCES

[1] H. Yin, S. Liu, Y. Feng, M. Li, J. Ren and H. Jiang, "Experimental Test Rig for Combustor-Turbine Interaction Research and Test Results Analysis," in Proceedings of ASME Turbo Expo 2015: Turbine Technical Conference and Exposition , Montréal, 2015.

[2] C. Wang, L. Wang, B. Sundén, V. Chernoray and H. Abrahamsson, "An Experimental Study of Heat Transfer on an Outlet Guide Vane," in Proceedings of ASME Turbo Expo 2014: Turbine Technical Conference and Exposition, Düsseldorf, 2014.

[3] J. F. Carrotte, K. F. Young and S. J. Stevens, "Measurements of the Flow Field Within a Compressor Outlet Guide Vane Passage," in International Gas Turbine and Aeroengine Congress and Exposition, Cincinnati, 1993.

[4] J. Larsson, V. Chernoray and S. Ore, "Effect of Geometry Deviations on the Aerodynamic Performance of an Outlet Guide Vane Cascade," in Proceedings of ASME Turbo Expo 2010: Power for Land, Sea and Air, Glasgow, 2010.

[5] Y. Huang, M. C. Leu, J. Mazumder and A. Donmez, "Additive Manufacturing: Current State, Future Potential, Gaps and Needs, and Recommendations," Journal of Manufacturing Science and Engineering, pp. 014001-1 - 014001-10, 2015.

[6] R. E. Laureijs, J. B. Roca, S. P. Narra, C. Montgomery, J. L. Beuth and E. R. H. Fuchs, "Metal Additive Manufacturing: Cost Competitive Beyond Low Volumes," Journal of Manufacturing Science and Engineering, vol. Vol. 139, pp. 081010-1 - 081010-9, 2017.

[7] O. Andersson, A. Graichen, H. Brodin and V. Navrotsky, "Developing Additive Manufacturing Technology for Burner Repair," Journal of Engineering for Gas Turbines and Power, vol. Vol. 139, pp. 031506-1 - 031506-9, 2017.

[8] B. Kirollos and T. Povey, "Laboratory Infrared Thermal Assessment of Laser-Sintered High-Pressure Nozzle Guide Vanes to Derisk Engine Design Programs," Journal of Turbomachinery, vol. Vol. 139, pp. 041009-1 - 041009-12, 2017.

[9] J. Schurb, M. Hoebel, H. Haehnle, H. Kissel, L. Bogdanic and T. Etter, "Additive Manufacturing Of Hot Gas Path Parts And Engine Validation In a Heavy Duty GT," in Proceedings of ASME Turbo Expo 2016: Turbomachinery Technical Conference and Exposition, Seoul, 2016.

[10] C. S. Cunningham, P. David Ransom, P. Jason Wilkes, J. Bishop and B. White, "Mechanical Design Features of a Small Gas Turbine for Power Generation in Unmanned Aerial Vehicles," in Proceedings of ASME Turbo Expo 2015: Turbine Technical Conference and Exposition, Montréal, 2015.

[11] V. A. Safronov, R. S. Khmyrov, D. V. Kotoban and A. V. Gusarov, "Distortions and Residual Stresses at Layer-by-Layer Additive Manufacturing by Fusion," Journal of Manufacturing Science and Engineering, vol. Vol. 139, pp. 031017-1 - 031017-6, 2017.

[12] M. P. Boyce, "Axial-Flow Compressors," in Gas Turbine Engineering Handbook, pp. 163-193.

[13] R. J. Monhardt, J. H. Richardson and J. M. Boettcher, "Design and Test of the FT8 Gas Turbine Low Pressure Compressor," in The Gas Turbine and Aeroengine Congress and Exposition, Toronto, 1989.

[14] Renishaw, Renishaw additive Manufacturing System AM250 - User Guide.

[15] M. Kniepkamp, J. Fischer and E. Abele, "Dimensional Accuracy Of Small Parts Manufactured By Micro Selective Laser Melting," in Solid Freeform Fabrication 2016: Proceedings of the 276th Annual International Solid Freeform Fabrication Symposium – An Additive Manufacturing Conference, Darmstadt, 2016.

[16] M. Thöne, S. Leuders, A. Riemer, T. Tröster and H. Richard, "Influence of heat-treatment on Selective Laser Melting products – e.g. Ti6Al4V," in Solid Freeform Fabrication Symposium, 2012.

[17] M. F. Zaeh and G. Branner, "Investigations on residual stresses and deformations in selective laser melting," Production Engineering - Research and Development, vol. 4, p. 35–45, 2010.

[18] P. Mercelis and J.-P. Kruth, "Residual stresses in selective laser sintering and selective laser melting," Rapid Prototyping Journal, vol. 12, no. 5, p. 254–265, 2006.

[19] J. Kruth, M. Badrossamay, E.Yasa, J. Deckers, L. Thijs and J. V. Humbeeck, "Part and material properties in selective laser melting of metals," in 16th International Symposium on Electromachining.

[20] O. Scott-Emuakpor, C. Holycross, T. George, K. Knapp and J. Beck, "Fatigue and Strength Studies of Titanium 6Al–4V Fabricated by Direct Metal Laser Sintering," Journal of Engineering for Gas Turbines and Power, pp. 022101-1 - 022101-7, 2016.

[21] T. Brajlih, B. Valentan, J. Balic and I. Drstvensek, "Speed and accuracy evaluation of additive manufacturing machines," Rapid Prototyping Journal, vol. 17, no. 1, pp. 64-75, 2011.

[22] M. B. Bauza, S. P. Moylan, R. M. Panas, S. C. Burke, H. E. Martz, J. S. Taylor, P. Alexander, R. H. Knebel, R. Bhogaraju, M. T. O'Connell and J. D. Smokovitz, "Study Of Accuracy Of Parts Produced Using Additive Manufacturing," Spring Topical Meeting, vol. 57, pp. 86-91, 2014.

[23] Y.-H. Pan, "Part height control of laser metal additive manufacturing process," Scholars' Mine, 2013.